Acta Crystallographica Section D
Biological Crystallography
ISSN 0907-4449

Crystallisation under microgravity of mistletoe lectin I from *Viscum album* with adenine monophosphate and the crystal structure at 1.9 Å resolution

R. Krauspenhaar, W. Rypniewski, N. Kalkura, K. Moore, L. DeLucas, St. Stoeva, A. Mikhailov, W. Voelter and Ch. Betzel

Crystallisation under microgravity of mistletoe lectin I from *Viscum album* with adenine monophosphate and the crystal structure at 1.9 Å resolution

R. Krauspenhaar[a], W. Rypniewski[a], N. Kalkura[a], K. Moore[b], L. DeLucas[b], St. Stoeva[c], A. Mikhailov[d], W. Voelter[c] and Ch. Betzel[a*]

[a]*Institute of Medical Biochemistry and Molecular Biology, University Hospital, c/o DESY, Build. 22a, Notkestr. 85, 22603 Hamburg, Germany,* [b]*Center for Macromolecular Crystallography, University of Alabama of Birmingham, Birmingham, AL35294-0005, USA,* [c]*Institute of Physiological Chemistry, University of Tübingen, Hoppe-Seyler-Str. 4, 72076 Tübingen, Germany, and* [d]*Institute of Crystallography of Russian Academy of Sciences, Leninsky Prospect 59, Moscow 117333, Russian Federation. E-mail: Betzel@unisgi1.desy.de*

The crystal structure of the ribosome-inactivating protein (RIP) mistletoe lectin I (ML-I) from *Viscum album* in complex with adenine has been refined to 1.9 Å resolution. High quality crystals of the ML-I complex were obtained by the method of vapour diffusion using the high density protein crystal growth system (HDPCG) on the international space station, mission ISS 6A. Hexagonal crystals were grown during three months under microgravity conditions. Diffraction data to 1.9Å were collected applying synchrotron radiation and cryo- techniques. The structure was refined subsequently to analyse the structure of ML-I and particularly the active site conformation, complexed by adenine that mimics the RNA substrate binding.

Keywords: ribosome-inactivation, microgravity, active site

PDB reference: 1M2T

1. Introduction

The heterodimeric glycoprotein ML-I is a ribosome-inactivating protein of type II and consists of a toxic A-chain which depurinates specifically the ribosomal 23S/28S rRNA, causing a total inactivation of protein biosynthesis in eukaryotic cells. The B-chain of RIP's type II is a product of a series of gene duplications (Villafranca & Robertus, 1981) and shows for ML-I distinct galactose-specific lectin activity. To analyse and describe the specific functional features of the glycosylation and sugar binding specificity we co-crystallised on the ground ML-I with lactose as well as with galactose and collected diffraction data up to 2.3Å (manuscript in preparation). The B chain is also able to bind to cell surface receptors and triggers the endocytotic uptake of the toxin into the cell. The overall protein fold of ML-I, as shown in Figure 1, is homologous to ricin from *Ricinus communis* (Monfort, *et al.*, 1987) and other known RIP type II proteins (Krauspenhaar *et al.*, 1999) with about 40% identity for the A-chain and 60% identity for the B chain (Eschenburg *et al.*, 1998). However, out of the family of ribosome-inactivating proteins only ML-I is a major component of therapeutically active substances present in commercially available mistletoe extracts applied in the treatment of human cancer. The A chain of ML-I conjugated to immunotoxins was shown to be even more active than immunotoxins with ricin A chain (Tonevitsky *et al*., 1996). Therefore the detailed analysis to high resolution, the comparison with other RIP type II proteins and to the known ML-I isoforms will provide new insights towards understanding the lectin as well as the cytotoxic activity. Further knowledge about the active site architecture will give more detailed information about RIP reaction mechanism and substrate recognition, which so far has not been described conclusively in the literature (Monzingo & Robertus, 1992; Endo & Tsurugi, 1988). In order to achieve the required quality of data for this analysis, it is necessary to obtain crystals of high quality. In a number of reported cases, superior crystals have been produced under microgravity conditions (Ng *et al*., 2002, Boggon *et al*., 1998, DeLucas *et al*., 1989). For this reason we have undertaken the current study.

2. Material and methods

2.1. Crystallisation and X-ray diffraction measurements

Mistletoe lectin I was purified following the previously described procedure (Franz *et al*., 1981) and concentrated for crystallisation to 7.5 mg/ml in 0.2 M glycin (Sigma) buffer adjusted to pH 2.5 with HCl. Crystals of ML-I complexes were obtained by vapour diffusion using the high density protein crystal growth system (HDPCG), supplied by NASA within its programme of crystal growth under microgravity on the international space station (mission ISS 6A). The HDPCG reaction chamber consists of a reservoir in which a suitable piece of chromex absorbent pellet was placed to suck the reservoir solution and a protein insert in which the protein droplet was equilibrated against the reservoir. The reservoir was filled with 500 µl of solution containing 32 % saturated ammonium sulphate in 0.1 M glycin/HCl buffer pH 2.5, 0.05 M adenosine 5'monophosphate (AMP) and in addition 20 µl of dioxan. The protein insert contained 20 µl of solution consisting of 10 µl of the protein solution and 10 µl of the reservoir solution. Crystallisation set-ups were launched on space shuttle mission STS 100 to the international space station. Once in orbit, the chambers were activated by a 180° rotation of the protein insert to connect it to the reservoir. The crystallisation experiment was performed at 20°C. The chambers stayed in space for approximately 110 days and then returned to earth on board mission STS 105. The crystals were retrieved from the HDPCG reaction chambers into a cryoprotectant solution containing 40% saturated ammonium sulphate, 0.1 M AMP and 30% glycerol in 0.1 M glycin/HCl buffer at pH 2.5. After approximately 1 min, the crystals were picked from the cryoprotectant solution with a cryo-loop (Hampton Research) and exposed quickly to a cold (100K) nitrogen gas. Frozen crystals were stored in liquid nitrogen. In the control experiment crystallisation set-ups were prepared in a similar way to the space experiment and activated over the same time period.

The diffraction experiment was performed at the EMBL beamline BW7B at the DORIS storage ring, DESY, Hamburg. X-ray intensity data were recorded on a MAR image plate scanner to a resolution of 1.9Å under cryogenic conditions. The X-ray wavelength was set to 0.8459 Å. The crystal was mounted with the *c*-axis approximately parallel with the goniometer rotation axis. This was necessary due to the very long unit cell length, which would result in an unacceptable number of reflection overlaps in any other crystal orientation. In total 209 images were collected with a oscillation range per image of 0.3°. The data were measured in two passes at different exposure times to cover the whole range of intensities. The exposure time per image for the high resolution pass was 230 s. The data were indexed, intensities were integrated and reduced to a unique set by using the programs DENZO and SCALEPACK (Otwinowski & Minor, 1997).

2.2. Refinement

The native ML-I structure, previously refined to 2.3Å (Krauspenhaar, unpublished) was used as the starting model in the refinement of the complex using the program CNS (Brünger & Rice, 1997). Subsequently the stereochemically restrained maximum-likelihood method (Murshudov *et al.*, 1997) was applied, as implemented in the program REFMAC from the *CCP*4 program suite, (CCP4, 1994). Data were used between 25 and 1.9 Å, without a σ cut-off, with 5% of the data set aside for R_{free} (Brünger, 1992). Solvent molecules were inserted and refined using the program ARP (Lamzin & Wilson, 1993) with real space positional refinement and automatic determination of statistically significant electron density level. Manual rebuilding of the model was based on the ($2F_o$-F_c) and (F_o-F_c) electron density maps, using Turbo-Frodo (Roussel & Cambillau, 1991) running on Silicon Graphics O2 workstation. The refinement was terminated when no further significant improvement could be achieved in R-factor statistics, model completeness and stereochemistry and electron density.

3. Results and discussion

3.1. The crystals

High quality hexagonal crystals were grown during the approximately 110 days under microgravity. The crystals reached the size 0.5 x 0.3 x 0.3 mm. For comparison, the crystals obtained in the control experiment on the ground were smaller than 0.1 mm – too small for mounting in the X-ray beam. The best crystals of ML-I ever obtained on the ground, in our laboratory, diffracted at best to 2.3 Å resolution. These crystals had been grown using a protein concentration of 10 mg/ml and the standard hanging drop method applying the same crystallisation conditions as described above. They grew in about 2 to 3 weeks at room temperature and reached the size between 0.1 and 0.3 mm in the longest dimension. The glycoprotein ML-I forms crystals with a large and asymmetric unit cell, along the *c*-axis (Table 1), and a high solvent content, 70 %. Under these circumstances the crystals grown in microgravity represent a significant improvement in size and quality, which in the end resulted in better data and improved resolution. Unfortunately, the crystallisation in the HDPCG reactors on earth produced numerous small crystals. The crystallisation process on the ground is faster than in orbit (Ng *et al.*, 2002) and it appears that the high rate of nucleation prevented formation of large crystals.

3.2. Refinement

The final model comprises 510 amino acid residues of ML-I, 541 water molecules, 1 adenine, 7 glycerol molecules and 8 saccharide residues at three glycosylation sites, indicated also in Figure 1. The final model of ML I has been assigned unit occupancy, except for a small number of regions at the surface of the A-chain, mainly loop regions, with substantial thermal motion or static disorder which is reflected in very weak density in the Fourier syntheses and higher values of the corresponding temperature factors. Disorder has been observed in the electron density for a region of 7 residues, from the intra-chain disulphide bridge to the C-terminus of the A-chain (Figure 1), and for the first 4 residues of the B-chain. These residues have been omitted in the current model. Refinement parameters are summarised in Table 1.

3.3. The overall structure

As shown in Figure 1 the toxic A-chain of ML-I is a globular enzyme with extensive secondary structure, accommodating the active site region. The B-chain corresponds to a lectin and is folded into two homologous domains containing multiple sugar binding

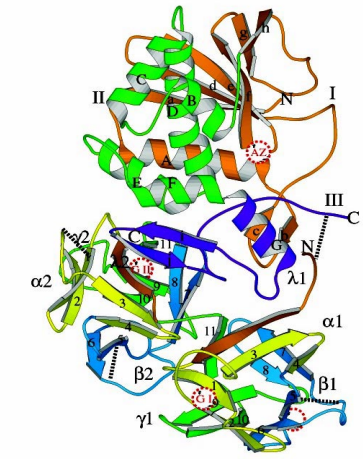

Figure 1

Cartoon plot of ML-I. The three domains of the A-chain are labeled I, II & III and coloured orange, green and turquoise. The helices of the secondary structure are labeled with capital letters, β-sheets in lowercase. For the B-chain the domains I and II are coloured according to their subdomains: The linker region λ1 and λ2 are shown in orange, the homologous subdomains α, β, γ are numbered in ascending order and coloured yellow, green and blue. The disulphide bond connecting the two chains is shown as dashed line. Dashed red circles indicate the active site region "AZ" at the A chain and the galactose-binding sites "G1" and "G2" in the B chain. The N and C terminus are indicated with "N" and "C".

sites to recognize and interact with specific glyco-structures on the surface of target cells. While the A-chain is composed of both, α and β secondary structure elements the B-chain consists only of β-sheets. The A-chain is divided in three globular domains. The B-chain is a product of a gene duplication, homologous subdomains and a so-called linker domain are arranged along a pseudo three fold axis and build up two domains. Both subunits are associated and stabilised by numerous non-covalent interactions across the interface region and linked by a disulfide bridge between residues Cys260A and Cys5B (Krauspenhaar *et al.*, 1999). A least-squares minimised superposition of the ML-I A-chain with the corresponding structure of ricin complexed with adenine (Weston *et al.*, 1994) gave an r.m.s. deviation of 0.82Å for 218 comparable Cα atoms, after omitting regions of insertions and deletions and pairs of atoms with coordinates deviating by more than 3 r.m.s. The major differences occur primarily in loop regions on the surface of the protein. A least-squares superposition and comparison of the unliganded (Krauspenhaar, unpublished) and adenine-bound ML-I A-chain gave an overall r.m.s. difference of 0.37 Å between Cα coordinates. The most significant changes upon binding of adenine occur within the active site, as discussed below.

3.4. The active site

The active site has N-glycosidase activity and deactivates eukaryotic ribosomes by depurinating a single adenine in a highly conserved rRNA GAGA-loop. The active site is located within the A-chain in a shallow cleft running along the surface of the protein and includes Tyr76A, Tyr115A, Glu177A and Arg168A, which are known to be the key residues in the catalytic process (Husain *et al.*, 1994; Monzingo & Robertus, 1992). The electron density indicates clearly that only adenine is bound in the active site, although AMP was used in the crystallisation. It is likely that the AMP has been hydrolysed by ML-I and that RIP activity is present in the crystal, as was shown

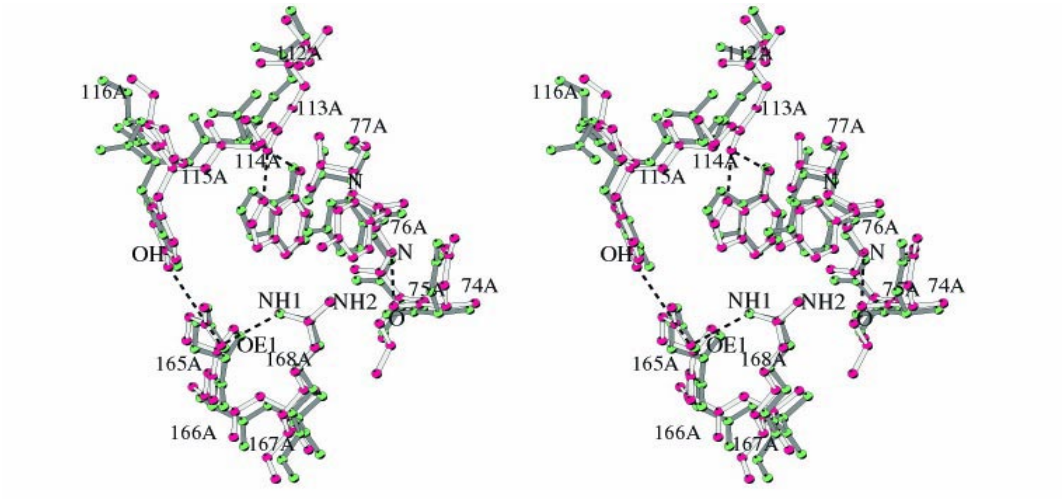

Figure 2

Superposition of the invariant active site residues of ricin shown in dark green and ML-I. The figures were drawn using MOLSCRIPT (Kraulis, 1991).

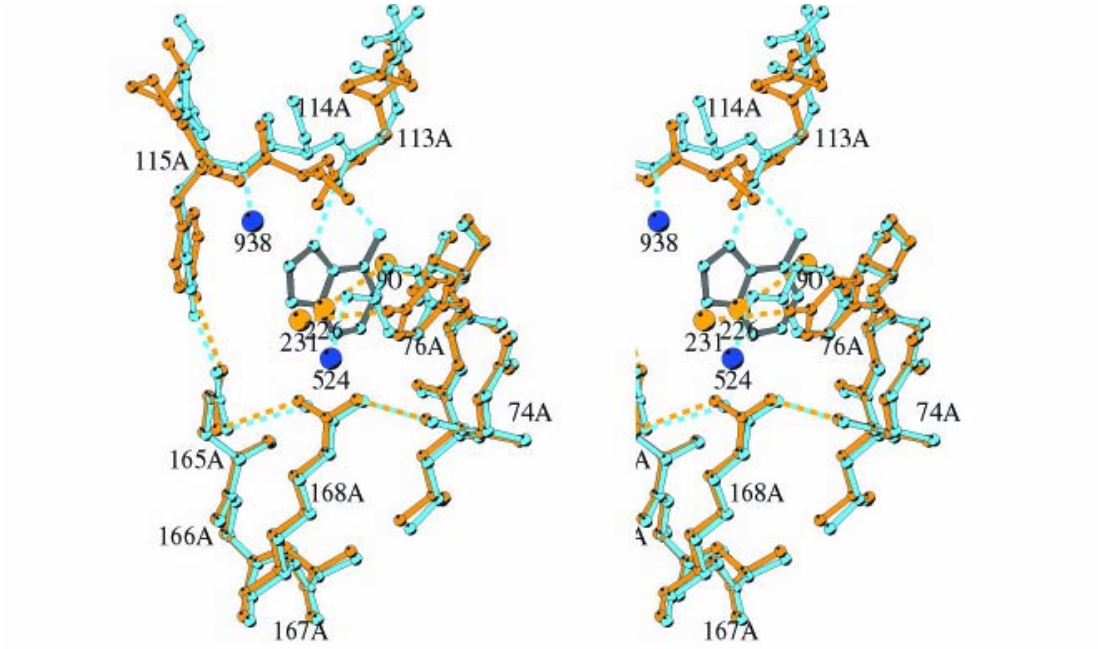

Figure 3

Stereo view of the active site of ML-I in native conformation as well in complex with adenine. Native ML-I is shown in yellow and with bound adenine in blue. Hydrogen bonds and water molecules are coloured according to the residues. The catalytic key residues for the *N*-glycosidase activity are: Tyr76A, Tyr115A, Glu177A and Arg168A.

for ricin by Weston *et al.* (1994). It is also possible that the low pH of the crystallisation buffer might also be factor in the hydrolysis of AMP. The architecture of the active site and the bound adenine is similar to the corresponding structure of ricin (Fig. 2) and indicates that the closed arrangement of the active site is conserved throughout the wide range of RIPs (Katzin *et al.*, 1991). A comparison of the active site between the unliganded lectin (Krauspenhaar, unpublished) and the adenine-bound enzyme shows several changes (Fig. 3): The side chain of Tyr 76A is rotated when adenine is bound and several water molecules are displaced from the active site. More extensive changes occur for residues 112A-118A which form a loop that is part of the adenine binding pocket, including Gly113A whose carbonyl oxygen forms a hydrogen bond to N6 and N7 of adenine. In the presence of adenine this loop is shifted by approximately 1Å to enlarge the binding pocket in order to accommodate the ligand. Both Arg168A and Glu165A, alternatively proposed as the activators for the hydrolytic water molecule (Monzingo & Robertus, 1992; Weston *et al.*, 1994), are present in their conserved positions in the vicinity of N9 of adenine, but only a weak water density is observed (Fig. 4b) nearby: 3.2 Å from N9, 4.0 Å from Nη1-Arg168A and 4.2 Å from Oε2-Glu165A. Thus the identity of the hydrolytic water molecule and its activating group remain unresolved in the present structure. The adenine is bound in a tight pocket at the active site *via* two types of interactions: non-polar and hydrogen bonds. The non polar interactions primarily involve aromatic ring-stacking on both sides

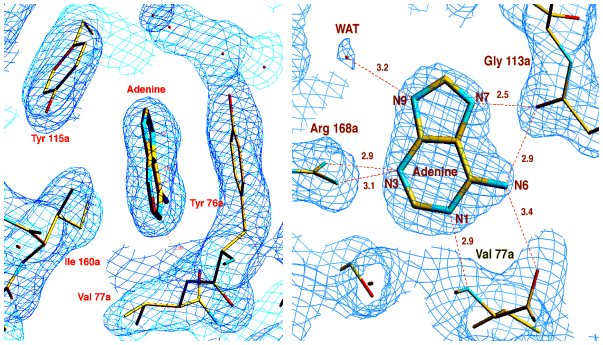

Figure 4
(2*Fo-Fc*) electron density in two orientations with superimposed amino acids and adenine at the active site. H-bonds and distances are labeled.

Table 1 Data collection and refinement parameters and statistics

unit cell	*a*=*b*= 107.1, *c*= 309.8 Å
space group	$P6_522$
X-ray source	beam line BW7B
resolution range	25.0 - 1.89 Å
total number of reflections	3,237,514
unique reflections	83,270
completeness	98.8 % (99.5 %)*
Overall % greater than 2σ	77.2
I/σ in high resol. bin	2.26
R-merge **	0.068
R-factor*** / R_{free}	0.21/0.24

* in high resolution bin: 1.93-1.89 Å
**R-merge = $\sum| I_i-\langle I\rangle |/\sum\langle I\rangle$, where I_i is an individual intensity measurement and <I> is the average intensity for this reflection, with summation over all data
*** R-factor = $\sum| F_o-F_c |/\sum| F_o |$

of the adenine plain (Figure 4a). A second type of stabilisation is achieved by hydrogen bonds around the edge of the adenine plane (Fig. 4b). The H-bonding potential of adenine is fully realised and although the hydrogen atoms cannot be observed directly at this resolution, the nature of the H-bonding can be inferred from the acceptor-donor geometry and distances. In particular, the hydrogen bonding distances between N7 of adenine and the carbonyl oxygen of Gly113A indicate the predominance of the adenine tautomer in which N7 is protonated. The extensive H-bonding of adenine may play a significant role in the reaction mechanism. The role of H-bonds as a form of partial protonation has been discussed before in this context (Monzingo & Robertus, 1992), as a means to facilitate the flow the electrons into the adenine ring, away from the glycosidic bond. Of particular significance in the present structure is the observation of the strong H-bond at the protonated N7 of adenine. The protonation of N7 has been proposed as a prerequisite in depurination reactions (Michelson, 1963). One outstanding question is the source of the proton, as there are no clear candidates for proton donors in the immediate vicinity. Nevertheless, it can be said that in the present structure the geometry of the adenine binding site is such that it favours the binding of the reaction product, where the H-bonding potential is fully realised with the tautomer of the adenine base protonated at N7, rather than with the substrate nucleotide, which is not protonated at N7.

Acknowledgments

This work is supported by the Deutsche Agentur für Luft und Raumfahrtangelegenheiten under Contract WB 509915 and via the RiNA GmbH, Berlin, Germany, the authors thank NASA for the opportunity to crystallise samples under microgravity.

References

Brünger, A and Rice, L. M. (1997). *Methods Enzymol.* **277**, 243-269.
Boggon, T. J., Chayen, N. E., Snell, E. H., Dong, J., Lautenschlager, P., Potthast, L., Siddons, D. P., Stojanoff, V., Gordon, E., Thompson, A. W., Zagalsky, P. F., Bi, R. C. & Helliwell, J. R. (1998). *Philos. Trans. R. Soc. London Ser. A*, **356**, 1045-1061.
Collaborative Computational Project, Number 4. (1994). *Acta Cryst.* D**50**, 760-763.
DeLucas, L. J., Smith, C. D., Smith, H. W., Vijay-Kumar, S., Senadhi, S. E., Ealick, S. E., Carter, D. C., Snyder, R. S., Weber, P. C., Salemme, F. R. *et al.* (1989). *Science*, **246**, 651-654.
Endo, Y. & Tsurugi, K. (1988). *J. Biol. Chem.* **263**, 8735-8739.
Eschenburg, S., Krauspenhaar, R., Mikhailov, A., Stoeva, St., Betzel, Ch. & Voelter, W. (1998). *Bioch. Biophys. Res. Commun.* **247**, 367-372.
Franz, H., Ziska, P. & Kindt, A. (1981). *Biochem. J.* **195**, 481-484.
Husain, J., Tickle, I. J. & Wood, S. P. (1994). *FEBS Lett.* **342**, 154-158.
Krauspenhaar, R., Eschenburg, S., Perbandt, M., Kornilov, V., Konareva, N., Mikailova, I, Stoeva, S., Wacker, R., Maier, T.,Singh, T., Mikhailov, A., Voelter, W. & Betzel, Ch. (1999). *Biochem.Biophys.Res.Commun.* **257**, 418-424.
Katzin, B. J., Collins, E. J. & Robertus, J. D. (1991). *Proteins Struct. Funct. Genet.* **10**, 251-259.
Kraulis, J. (1991). *J. Appl. Cryst.* **24**, 946-950.
Michelson, A.M. (1963). *The Chemistry of Nucleosides and Nucleotides*, Academic Press, London
Monfort, W., Villafranca, J. E., Monzingo, A. F., Ernst, S., R., Katzin, B., Rutenber, E., Xuong, N. H., Hamlin, R. & Robertus, J. D (1987) *J. Biol.Chem.* **262**, 5398-5403.
Monzingo, A. F. & Robertus, J. D. (1992). *J. Mol. Biol.* **227**, 1136-1145.
Murshudov, G. N., Vagin, A. A. & Dodson, E. J. (1997). *Acta Cryst.* D**53**, 240-255.
Ng, J. D., Sauter, C., Lorber, B., Kirkland, N., Arnez, J. & Giegé, R. (2002) *Acta Cryst.* D**58**, 645-652.
Otwinowski, Z. & Minor, W. (1997). *Methods Enzymol.* **276**, 307-326.
Roussel, A. & Cambillau, C. (1991). *Silicon Graphics Geometry Patners Directory 86*, Silicon Graphics, Mountain View, CA.
Tonevitsky, A. G., Agapov, I. I., Abdijapar, T. S., Temyakov, D. E., Pohl, P. & Kirpichnikov, M. P. (1996). *FEBS Lett.* **392**, 166-168.
Villafranca, J. E. and Robertus, J. D. (1981). *J. Biol. Chem.* **256**, 554-556
Weston, W. A., Tucker, A. D., Tchacher, D. R., Derbyshire, D. J. & Pauptit, R. A. (1994). *J. Mol. Biol.* **244**, 410-422.